IDAHO GEOLOGICAL SURVEY MOSCOW
MONTANA BUREAU OF MINES AND GEOLOGY

IDAHOGEOLOGY.ORG
MBMG.MTECH.EDU

DIGITAL WEB MAP 230
MBMG GEOLOGIC MAP 103
STEWART AND OTHERS

GEOLOGIC MAP OF THE LOST TRAIL PASS QUADRANGLE, LEMHI COUNTY, IDAHO, AND BEAVERHEAD AND RAVALLI COUNTIES, MONTANA

David E. Stewart, Reed S. Lewis, Jeffrey D. Lonn, Raymond Salazar, Russell F. Burmester, and Colleen Elliott

2025

https://doi.org/10.59691/LQOA5158

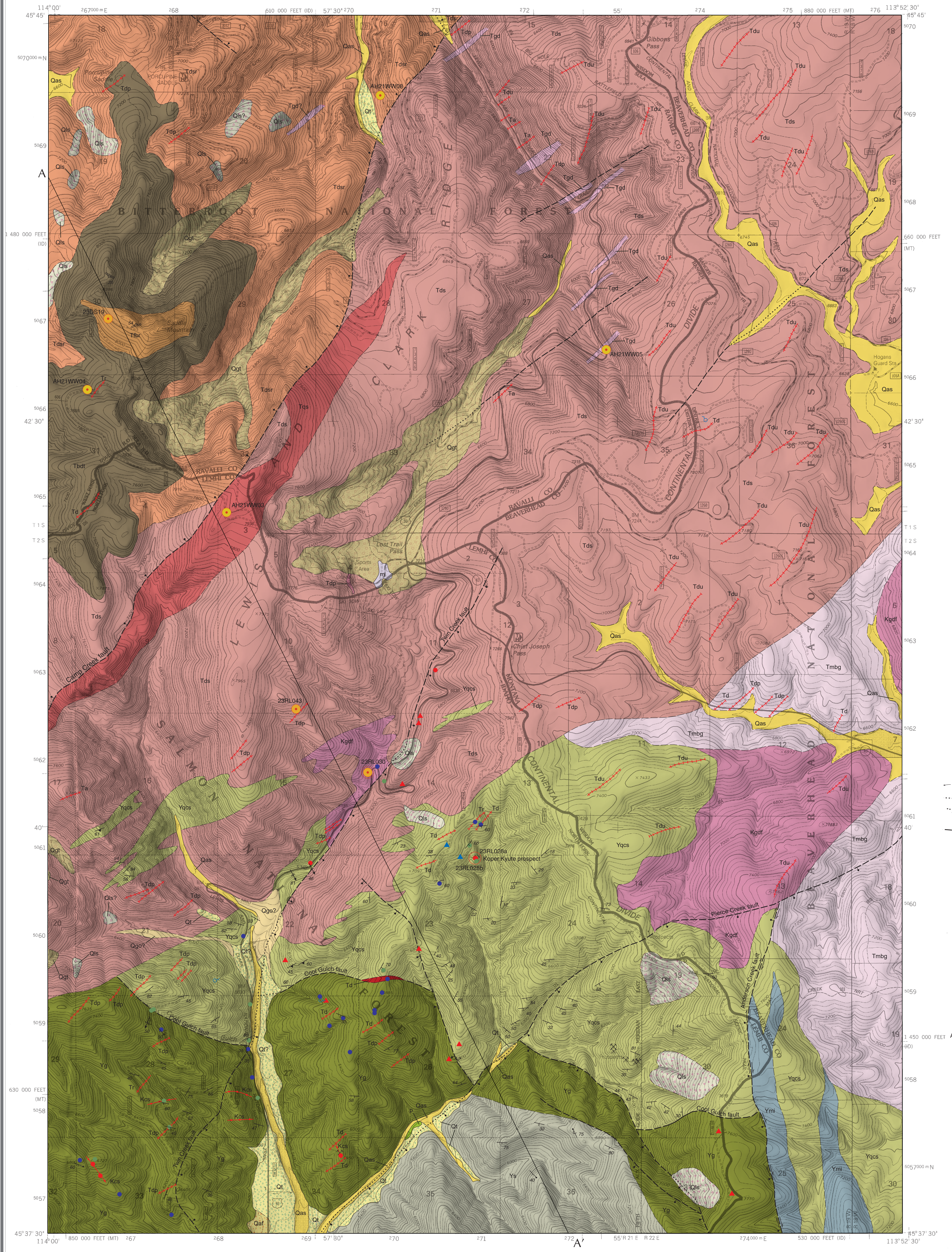

Base Map Credit

Topographic base modified from digitally scanned 1:24,000-scale USGS paper map, compiled from aerial photographs taken in 1965. Planimetry derived from imagery taken 1994.

Transverse Mercator projection. 1927 North American Datum.

10,000-foot grid ticks: State Plane Coordinate System, Idaho central zone.

1000-meter grid ticks: Universal Transverse Mercator, zone 12.

Montana coordinate system, south zone (Lambert conformal conic).

Shaded relief from 10 m DEM.

Declination from NOAA National Geophysical Data Center.

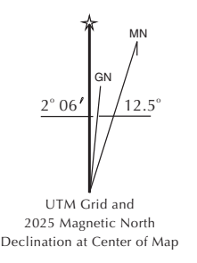

UTM Grid and 2025 Magnetic North Declination at Center of Map

SCALE 1:24,000

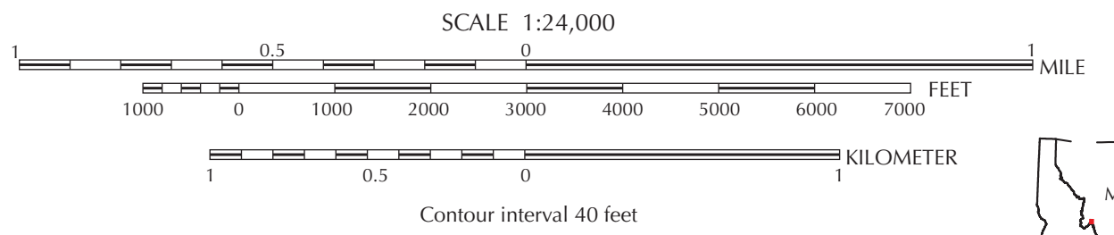

Contour interval 40 feet

QUADRANGLE LOCATION

ADJOINING QUADRANGLES

Field work conducted in 2011, 2012, and 2023.

This geologic map was funded in part by the U.S. Geological Survey National Cooperative Mapping Program, U.S.G.S. Award No. G23AC00405. The views and conclusions contained in this document are those of the authors and should not be interpreted as necessarily representing the official policies, either expressed or implied, of the U.S. Government.

GIS and digital cartography by David Vohra and Jonathan Sandquist at the Idaho Geological Survey's Digital Mapping Lab.

Technical review by Dennis Feeney and Claudio Berti.

Map version 05-30-2025.

GIS data and PDF of this map can be downloaded from www.idahogeology.org.

CORRELATION OF MAP UNITS

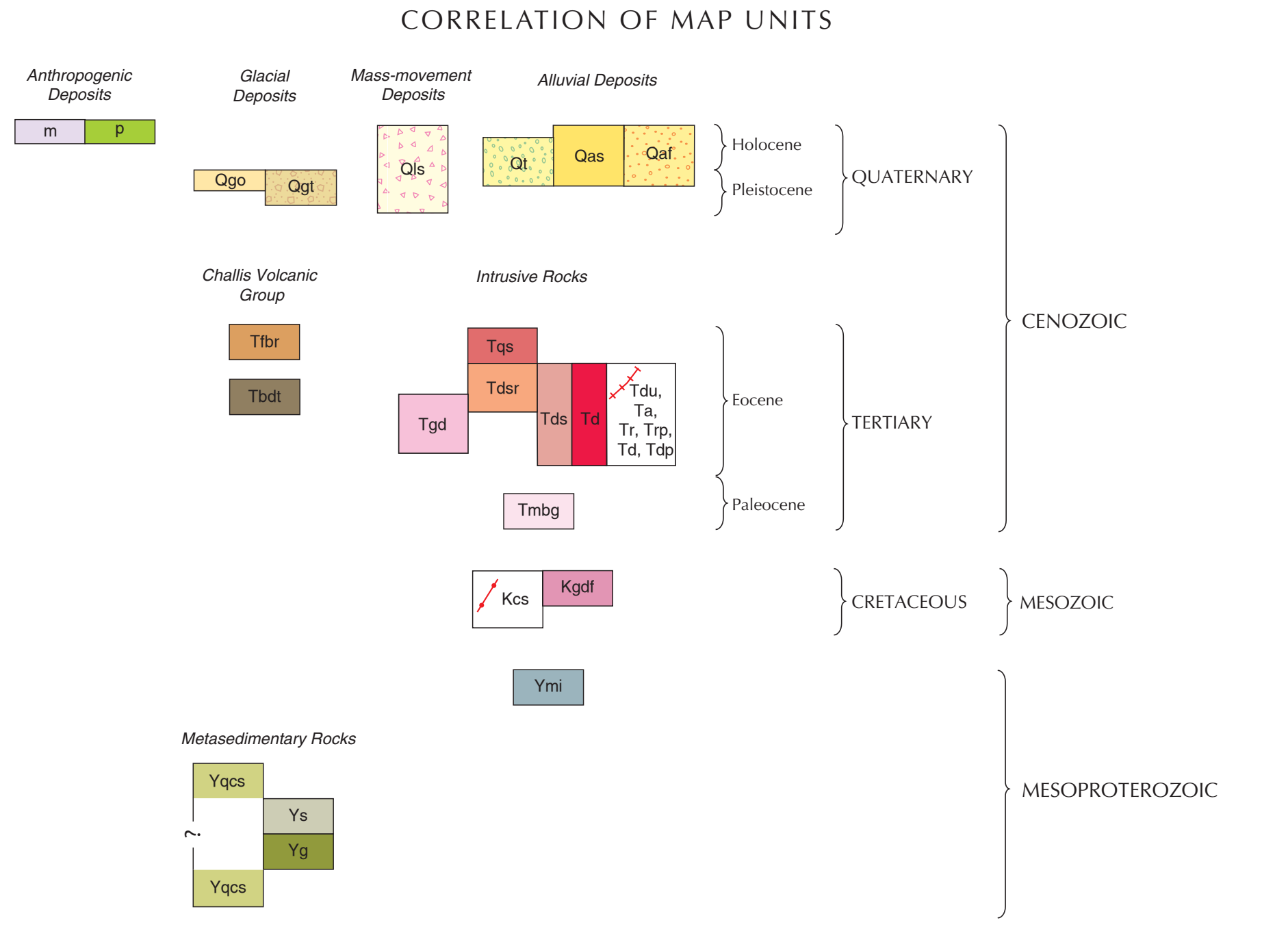

INTRODUCTION

The map is the result of field work primarily in 2011, 2012, and 2023, and previous research in the region. Field sheets from the 2011 and 2012 mapping by Eric and David Stewart that were used to produce a 1:40,000 scale regional map (Stewart and others, 2014) were indispensable in producing the present map. Previous regional mapping also includes Desmarais (1983) at 1:50,000 scale and Evans and Green (2003) at 1:100,000 scale. Many concepts for geologic units were developed while mapping in the Beaverhead Mountains to the southeast as part of a 1:24,000-scale collaborative mapping project by the Idaho Geological Survey and the Montana Bureau of Mines and Geology that started in 2007 and resulted in geologic maps of the western (Burmester and others, 2016a) and eastern (Lonn and others, 2019) parts of the Salmon 30' x 60' quadrangle (orange outline, Figure 1) southeast of this map (blue outline, Figure 1). Mapping of landslides, alluvial deposits, placer deposits, and glacial deposits was aided by LiDAR-derived hillshade images. Magnetic susceptibilities were measured with KT-9 and KT-10 Kappameters from Exploranium G.S. Ltd. and Terraplus Inc., typically on 10 measurements per exposure and averaged (Table 1). Results are summarized as a histogram in Figure 2. U-Pb zircon ages on four samples collected in 2023 were analyzed by staff at the Montana Bureau of Mines and Geology (MBMG). Results are plotted in Figure 3. Locations for 2021 sampling at four localities by MBMG and reported by Mosolf and Kylander-Clark (2023b) are also shown on the map.

The oldest rocks in the quadrangle are Mesoproterozoic metasedimentary rocks. They are intruded by Mesoproterozoic mafic rocks and Cretaceous and Eocene granitic plutonic and subvolcanic dike rocks and are overlain by volcanic rocks of the Challis Volcanic Group and coeval sediments. Glacial deposits are present at higher elevations.

LOCATION OF FIELD OBSERVATIONS

Lost Trail Pass Quadrangle

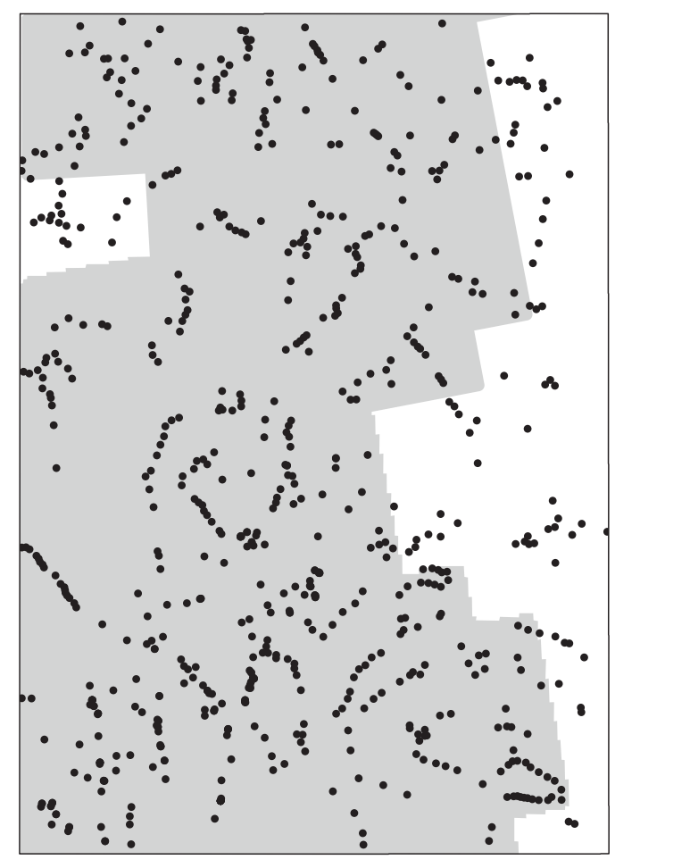

Extent of LiDAR coverage as of 08/2023

SYMBOLS

Contact: solid where certain; dashed where approximately located.

Fault: dashed where approximately located; dotted where concealed.

Normal fault: dashed where approximately located; dotted where concealed; ball and bar on downthrown side.

Reactivated right-lateral strike-slip fault with later normal motion: dashed where approximately located; arrows show relative lateral motion; ball and bar on downthrown side.

35 Strike and dip of bedding.

25 Approximate strike and dip of bedding.

15 Strike and dip of bedding known to be upright based on sedimentary structures.

30 Strike and dip of bedding known to be overturned based on sedimentary structures.

40 Strike and dip of foliation.

50 Strike and dip of eutaxitic foliation.

35 Bearing and plunge of minor fold axis.

20 Bearing and plunge of crenulation lineation.

▲ Tectonic breccia.

▲ Tourmaline breccia.

⚒ Prospect.

Spring.

23RL028a ◉ Geochemical sample location (Table 2).

23DS19 ◉ Geochronological sample location (Figure 3).

AH21WW04 ◉ Geochronological sample location (Mosolf and Kylander-Clark, 2023a).

Location of magnetic susceptibility measurement (Table 1).

- ● 0.02 - 0.20
- ● 0.21 - 1.00
- ● 1.01 - 10.00
- ● > 10.00

DESCRIPTION OF MAP UNITS

The geologic map of the Lost Trail Pass quadrangle shows rock units exposed at the surface or underlying a thin surficial cover of soil and colluvium. Igneous rocks are classified using International Union of Geological Sciences nomenclature (Le Bas and Streckeisen, 1991). Grain size classification of unconsolidated and consolidated sediment employs the Wentworth scale (Lane, 1947). Bedding thicknesses and lamination type are after McKee and Weir (1953). Time scale is the 2022 Geological Society of America version 6.0 (Walker and Geissman, 2022). Grain sizes and bedding thicknesses are given in abbreviation of metric units (e.g., dm=decimeter). Unit thicknesses, distances, and elevations are in both metric and English units. Multiple lithologies within a rock unit description appear in order of decreasing abundance, and descriptions of stratigraphic units are from bottom to top where possible

ANTHROPOGENIC DEPOSITS

m **Made ground (late Holocene)**—Disturbed ground and fill in the vicinity of the Lost Trail Pass ski lodge area.

p **Placered ground (late Holocene)**—Small areas of terraces along Pierce Creek that were placer mined for gold (Lorain and Metzger, 1939).

ALLUVIAL DEPOSITS

Qas **Side-stream alluvium (Holocene to Late Pleistocene)**—Subangular to rounded, moderately sorted and stratified pebble to boulder sandy gravel. Designated as 'Qas' as these are tributaries to the Salmon River.

Qaf **Alluvial-fan and debris-flow deposits (Holocene to Late Pleistocene)**—Angular to subrounded, poorly sorted, matrix-supported pebble to boulder gravel in a sand, silt, and clay matrix.

Qt **Terrace deposits (Holocene to Late Pleistocene)—**Subangular to rounded, moderately sorted and stratified pebble to boulder sandy gravel above current stream level along the North Fork of the Salmon River, Pierce Creek, and the West Fork of Camp Creek. Upper surface is relatively smooth and flat. Locally grade upstream into *Qgo* deposits. Includes single high gravel deposit north of Cool Gulch that is older and possibly Tertiary in age.

GLACIAL DEPOSITS

Qgo **Outwash (Late Pleistocene)**—Low areas of poorly sorted sand, gravel, cobbles, and boulders downstream from till deposits. Upper surface is steeper and less even than *Qt* deposits, but *Qgo* deposits grade into *Qt* deposits downstream so contacts between the two are approximate.

Qgt **Till deposits (Pleistocene)**—Unsorted sand, gravel, cobbles, and boulders. Clasts are subangular to subrounded or faceted. Forms end and lateral moraines with ground till in basins.

MASS-MOVEMENT DEPOSITS

Qls **Landslide deposits (Holocene to Pleistocene)**—Unstratified, unsorted silty clay, gravelly silty clay, and boulders.

CHALLIS VOLCANIC GROUP

Rocks of the Eocene Challis Volcanic Group formed from eruptions and to a lesser extent sedimentation. They are widespread to the south where they were mapped by D.H. McIntyre, E.B. Ekren, and R.F. Hardyman in the Challis 1° x 2° quadrangle (Fisher and others, 1992). Here only remnants of originally more extensive volcanic units are present.

Tfbr **Flow-banded rhyolite (Eocene)**—Light tan to pinkish-gray flow-banded, largely aphyric rhyolite (Figure 4). Crystal content generally sparse (less than 1 percent) but locally as much as 15 percent of quartz and potassium feldspar less than 1 mm in size. Trace amounts of biotite and hornblende present locally. Trace orange pumice as large as 2 mm, and lithics identical to matrix as large as 6 mm. Contains rare lithophysae. Lower two thirds of unit is pervasively flow-banded on a mm scale with banding highly distorted at some localities. Upper one third displays less distinct flow-banding. Weathers to form plates along welding surfaces. Presence of pumice and lithics, and local distortion of flow-banding, suggest this deposit was a hot ash-flow tuff that flowed after emplacement. No dikes were observed cutting this unit. Sample 23DS19 from northwest of Lost Trail Pass was dated by U-Pb LA-MC-ICP-MS methods on zircon and returned an age of 49.3 ± 0.2 Ma (Figure 3A).

Tbdt **Biotite dacite tuff (Eocene)**—Light-gray to tan, moderately welded dacitic ash to lapilli tuff (Figure 5). Characterized by dark quartz crystals as large as 3 mm and sparse but ubiquitous crystals of biotite and hornblende smaller than 1 mm. Heterogeneous with varied proportions of crystals, lithics, and pumice. Crystals, which comprise 10 to 30 percent, are predominantly white plagioclase as large as 5 mm. Subordinate quartz is commonly dark and as large as 3 mm. Pseudohexagonal biotite and acicular hornblende, as much as 3 percent, are small (<1 mm). Rounded volcanic lithics as large as 6 cm, similar to matrix but lighter in color, comprise from 0 to 40 percent of the rock. Rounded pumice as large as 1 cm is rare but locally comprises 20 percent of the unit. This tuff rests on an eroded surface of *Tdsr* and is cut by both rhyolite and dacite dikes. Mosolf and Kylander-Clark (2023b) reported a U-Pb zircon age of 52.2 ± 0.4 Ma for a sample collected southwest of Saddle Mountain (sample AH21WW04). That sample contained 70.83 percent SiO_2 (Mosolf and others, 2023).

INTRUSIVE ROCKS

Tqs **Quartz syenite (Eocene)**—Single large dike in northwest part of map that was injected along, and later cut by, the Camp Creek fault. Termed the Saddle Mountain quartz syenite by Desmarais (1983) who noted that rock was composed of ~75 percent perthitic potassium feldspar, ~15 percent plagioclase, ~7 percent quartz, and lesser amounts of amphibole, biotite, pyroxene (aegirine/aegirine-augite), and opaque oxides that includes magnetite cubes as large as 0.5 mm. Texture ranges from coarse-grained equigranular to porphyritic with potassium feldspar phenocrysts. Textural and compositional variation indicates multiple injections of magma. Dated at 49.3 ± 0.2 Ma (n = 38; MSWD = 0.8), using LA-MC-ICP-MS methods (sample AH21WW03 in Mosolf and Kylander-Clark, 2023b; see Symbols). SiO_2 content at dated locality is 64.08 percent (Mosolf and others, 2023).

Tdsr **Rhyolite dike swarm (Eocene)**—Area of abundant rhyolite dikes and subordinate dacite dikes. Over 90 percent of this unit is rhyolite to rhyolite porphyry dikes, with minor dacite or dacite porphyry dikes and very rare *Tgd* country rock screens. See dike descriptions below for individual lithologies. *Tdsr* does not crop out as well as *Tds*, but where exposed dikes are tabular, less than 15 m (50 ft) thick, and are sub-vertical with northeast strikes. Along U.S. Highway 93 in Montana immediately north of the map boundary *Tdsr* is weathered to low, pinkish slopes that contrast sharply with the resistant dikes of *Tds* to the south. Date of 51.2 ± 0.4 Ma reported in Mosolf and Kylander-Clark, (2023b; sample AH21WW08) for a dike near the northern map boundary that contains embayed quartz phenocrysts 2 to 4 mm across and altered potassium feldspar(?) phenocrysts 5 to 8 mm in length. SiO_2 content of that sample is 67.01 percent (Mosolf and others, 2023). Mapped as a rhyolite to rhyodacite dike swarm by Desmarais (1983).

Tds **Dike swarm (Eocene)**—Mixed unit consisting of dacite dikes and small stocks, rhyolite dikes, and minor amounts of country rock. Over 90 percent of this unit is dacite, dacite porphyry, rhyolite, and rhyolite porphyry dikes in roughly equal proportions; the remainder is country rock. See dike descriptions below for individual lithologies. The dike swarm is well exposed along U.S. Highway 93 near the northern map boundary. Dikes are parallel, tabular bodies as thick as 15 m (50 ft) that strike northeast and dip 70 degrees to the southeast. Cross-cutting relationships are rare. The exception is aphyric andesite dikes (*Ta*), only locally mapped, that appear to be late-stage intrusions. Similarity of dike composition, highly varied texture, rarity of chilled margins, and similar dike geometry, are consistent with injection from multiple magma chambers, possibly with magma mixing, over a relatively short time span. Porphyritic dacite (Figure 6; 23RL043) from southwest of Lost Trail Pass was dated by U-Pb LA-MC-ICP-MS methods on zircon and returned an age of 52.7 ± 0.3 Ma (Figure 3B). This sample is from an area of abundant dacite and is either a small stock or a large dike. Country rock within *Tds* is rare. North of Lost Trail Pass rare screens of *Tgd* or *Tmbg* separate dikes; south of the pass rare screens of *Yqcs*, *Tgd*, *Tmbg*, and *Kgdf* are within *Tds*. Dacite dikes grade into granodiorite (*Tgd*), which is locally mapped separately. Mapped in part as biotite granodiorite by Desmarais (1983).

Tgd **Granodiorite (Eocene)**—Fine- to medium-grained, equigranular to porphyritic biotite- and hornblende-biotite granodiorite. Grades into *Tds* where groundmass is very fine grained. Small exposure in roadcut along U.S. Highway 93 dated at 52.4 ± 0.2 Ma (n = 27; MSWD = 0.9), using LA-MC-ICP-MS methods (sample AH21WW05 in Mosolf and Kylander-Clark, 2023b; see Symbols). Sample contains embayed quartz phenocrysts 2 to 4 mm across and feldspar phenocrysts mostly 3 to 5 mm in length. SiO_2 content in that sample is 68.21 percent (Mosolf and others, 2023). That locality is slightly coarser grained and more equigranular than typical of *Tgd*.

Tdu **Dikes, undivided (Eocene)**—Dacite and rhyolite dikes forming resistant ribs.

Ta **Andesite dikes (Eocene)**—Sparsely porphyritic andesitic dikes. Phenocrysts are plagioclase, biotite, and hornblende.

Tr **Rhyolite dikes (Eocene)**—Rhyolite dikes with sparse quartz and potassium feldspar phenocrysts. Magnetic susceptibility at one exposure is 0.19×10^{-3} SI.

Trp **Porphyritic rhyolite dikes (Eocene)**—Gray to pinkish-gray highly porphyritic rhyolite dikes with conspicuous potassium feldspar phenocrysts. Phenocrysts that comprise as much as 60 percent of the rock are white plagioclase as large as 4 mm, lesser clear quartz as large as 5 mm, and pink euhedral potassium feldspar as large as 15 mm.

Td **Dacite dikes (Eocene)**—Dacite dikes with sparse plagioclase, quartz, hornblende, and biotite phenocrysts. Proportions of phenocrysts vary. Texture spans from nearly aphyric to nearly phaneritic, which closely resembles *Tgd*. Magnetic susceptibility at two exposures is 0.18×10^{-3} SI.

Tdp **Porphyritic dacite dikes (Eocene)**—Highly porphyritic dacite dikes with plagioclase, quartz, hornblende, and biotite phenocrysts. Proportions of phenocrysts vary. Textures range from highly porphyritic to nearly equigranular, which closely resembles that of *Tgd*. Magnetic susceptibility at two exposures is 0.21×10^{-3} SI.

Tmbg **Muscovite-biotite granite (Paleocene)**—Massive muscovite-biotite granite to granodiorite. Locally sparsely porphyritic with potassium feldspar phenocrysts. Minor to trace amounts of muscovite. Pegmatite and leucocratic granite are present locally. Desmarais (1983) mapped this as the Trail Creek pluton, which is more extensive east of this map. He reported weakly zoned plagioclase (An28-30) and common myrmekite. SiO_2 content of sample collected 7 km (4 mi) to the east-southeast in the Big Hole Pass quadrangle is 71.6 percent (sample 22RB402, Table 2). Magnetic susceptibility of two exposures is 0.21 and 0.48×10^{-3} SI. Locality along State Highway 43 12 km (7 mi) east of the quadrangle dated by U-Pb methods at 63.3 ± 0.6 Ma (sample CE20BHB15 in Mosolf and Kylander-Clark, 2023a).

Kgdf **Foliated granodiorite (Cretaceous)**—Foliated to massive biotite granodiorite (Figure 7). Anhedral and relatively large biotite (1-4 mm). SiO_2 content is 69.7 percent (23RL030, Table 2). That sample from exposure on U.S. Highway 93 southwest of Lost Trail Pass was dated by U-Pb LA-MC-ICP-MS methods on zircon and returned an age of 76.8 ± 0.4 Ma (Figure 3C). Magnetic susceptibility at that locality is 1.21×10^{-3} SI. Unit is older and more mafic than *Tmbg* and possibly correlative with the Martin Creek pluton of Desmarais (1983) that has been dated at about 78 Ma (but with a large error) on two samples.

Kcs **Calc-silicate veins (Cretaceous?)**—Red-brown weathering coarse-grained actinolite-diopside-calcite veins or dikes. Contacts sharp and linear (Figure 8). Median magnetic susceptibility measured at four exposures (one was three hand samples) is 8.77×10^{-3} SI. Known only in *Yg* in southwest corner of map and south-adjacent Gibbonsville quadrangle (Stewart and others, in prep). Possibly derived from remobilization of carbonate within structurally or stratigraphically underlying *Yqcs*.

Ymi **Mafic intrusive rocks (Mesoproterozoic)**—Fine- to medium-grained mafic dikes in southeast part of quadrangle. White plagioclase as much as 30 percent. Original hornblende and pyroxene partly altered to amphibole, chlorite, and epidote, likely during metamorphism. Western dike appears to have intruded along and subsequently been cut by the Anderson Creek fault. Sample 22RB406 collected near the state line 530 m (1,700 ft) south of the quadrangle was dated by U-Pb LA-MC-ICP-MS methods on zircon. Zircon yield from this sample was poor. Of nine grains analyzed, seven yielded similar ages with a $^{207}Pb/^{206}Pb$ weighted mean of 1264 ± 15 Ma (Figure 3D). One concordant (likely inherited) grain yielded a ~1747 Ma age and one discordant grain showed Cretaceous or younger Pb-loss. The same sample contained 52.7 percent SiO_2. A sample from a smaller mafic dike of uncertain age collected 10 km (6 mi) to the southeast of the quadrangle contained 50.8 percent SiO_2 (sample 22LK008, Table 2).

METASEDIMENTARY ROCKS

Mesoproterozoic metasedimentary rocks comprise most of the bedrock in the southern part of the quadrangle. They were metamorphosed to biotite grade but vary in grain size and biotite content. Unit names follow the stratigraphic nomenclature (Burmester and others, 2016b) that uses the coarsest unit, the Swauger Formation, to distinguish otherwise similar rocks that are present above and below it.

Ys **Swauger Formation (Mesoproterozoic)**—Light-gray to white, fine- to medium-grained, poorly-sorted quartzite with more feldspar, as much as 50 percent, than typical for this unit; potassium feldspar typically greater than plagioclase. Where mapped as Swauger Formation undivided (Ys of Stewart and others, 2014) quartzite beds generally fine upward within laterally continuous beds between 75 and 150 cm thick. Some cross-beds are defined by heavy mineral laminae with hematite. Approximately 3,400 m (11,000 ft) thick in the Allan Mountain quadrangle to the south (Stewart and others, 2014).

Yg **Gunsight Formation (Mesoproterozoic)**—Quartzite, siltite, and minor argillite. Mapped as Gunsight Formation by Stewart and others (2014) and described as gray, gray-green, and tan, well sorted, fine-grained feldspar-rich quartzite. Features include abundant heavy mineral laminations and soft-sediment deformation. The quartzite is well sorted, and is laminated to thinly bedded, commonly showing ripples, climbing ripples, load casts, and trough and planar cross-bedding. Median magnetic susceptibility measured at seven exposures and ten hand samples is 0.10×10^{-3} SI. Upper contact gradational above approximately 400 m (1,300 ft) of green to light gray, siltite to fine-grained quartzite (Stewart and others, 2014). Thickness on the map uncertain but estimated to be approximately 4,500 m (15,000 ft) (Stewart and others, 2014). Stratigraphic position under the Swauger Formation supports assigning this unit to the highest unit of the Lemhi Group.

Yqcs **Quartzite and calc-silicate rocks (Mesoproterozoic)**—Quartzite, siltite, calc-silicate rocks, and minor schist and phyllite. Bedding on cm to dm scale (Figure 9). Decreasing abundance of calc-silicate rocks northward, interpreted to be stratigraphically downward. Includes phyllite, schist, and gneiss in the northern and eastern exposures near contacts with plutonic rocks. Calc-silicate rocks are resistant to weathering and commonly crop out. They contain abundant actinolite along with plagioclase and local scapolite. Median magnetic susceptibility measured at eight exposures and two hand samples is 0.25×10^{-3} SI. Susceptibility was higher for two exposures within *Tds*: 4.18×10^{-3} SI. Thickness unknown as no lower or upper stratigraphic contact has been found, but a minimum of 1,000 m (3,280 ft) is likely. Previously mapped as calc-silicate, quartzite, and siltite of Dahlonega Creek (Stewart and others, 2014). If stratigraphically below *Yg*, lithologies suggest correlation with the Yellow Lake Formation, which contains carbonate, and possibly parts of the Big Creek Formation, largely very fine grained quartzite and siltite, both of the Lemhi Group (Burmester and others, 2016b). A similar stratigraphic level within strata mapped as the Yellowjacket Formation also contains carbonate (Ekren, 1988). Alternatively, could be below those units if normal displacement on the Cool Gulch fault was very large, perhaps the Piegan Group, mapped 14 km (9 mi) and 35 km (22 mi) northeast of this map (Elliott and Lonn, in prep.). Another possible correlative if the Cool Gulch and Anderson Creek faults had an earlier thrust history is the quartzite, argillite, and minor calc-silicate mapped above the Swauger Formation in the West Pioneer Mountains to the east (Lonn and Scarberry, 2022). However, that unit has medium quartz grains typical of the Lawson Creek Formation (Hobbs, 1980) that are absent in *Yqcs*.

STRUCTURE

This map and the Gibbonsville quadrangle to the south (Stewart and others, 2014; Stewart and others, in prep) share *Ys*, *Yg*, *Yqcs*, *Ymi*, *Kcs*, and the Anderson Creek fault. The Cool Gulch fault and the Lick Creek fault (on the Gibbonsville map) are the southern contacts of *Yqcs* with *Yg* or *Ys*. Understanding the local structure therefore depends on both maps. The general map pattern of Mesoproterozoic units west of the Anderson Creek fault is of a southward dipping homocline, with *Yqcs* under *Yg* under *Ys*. In the few outcrops where we were able to determine top directions, all strata were south to southwest facing. Although *Yg* is separated from *Yqcs* by the Cool Gulch fault, *Yqcs* could be stratigraphically below *Yg* if the fault were minor and only omitted part of a homoclinal section.

TWIN CREEK FAULT

The Twin Creek normal fault in the southwest part of the map can be traced 14 km (9 mi) south through the Gibbonsville quadrangle where it was first mapped (Stewart and others, 2014; Stewart and others, in prep). In the Gibbonsville quadrangle it places Challis Volcanic Group strata in the east against Mesoproterozoic metasedimentary rocks in the west. Brecciated fault rock at the mouth of Cool Gulch is attributed to this structure. The northern extent beyond Cool Gulch is uncertain.

COOL GULCH FAULT

The Cool Gulch fault, formerly the northern offset western segment of the Lick Creek fault (Stewart and others, 2014), is the contact between *Yg* and *Yqcs* in the southwestern part of the map. Here the Cool Gulch and Lick Creek faults are given separate names because of uncertainty that they are the same structure. Because of the uncertainty in the stratigraphic position of the *Yqcs* unit, several options exist for the nature of this contact. If *Yqcs* is older than *Yg* (middle to lower Lemhi Group) then it is likely a minor down-to-the-south normal fault. If *Yqcs* is younger than *Yg* and *Ys*, and equivalent to the Lawson Creek and Apple Creek formations, then it is a major structure. An exposure west of the North Fork Salmon River contains 50° south-southwest plunging structures that look like tight folds with amplitudes on the cm scale (Figure 10) in steeply dipping, thinly bedded quartzite with thinner schistose tops. Whether this deformation records faulting or folding is unclear. To the east the fault is offset by the Twin Creek fault and other normal faults so appears older than those, the intrusive rocks to the northwest, and *Td* that intrudes it east of the Twin Creek fault. It appears to cut out *Yg* eastward. The fault terminates at the Anderson Creek fault, which must have offset it or accommodated its displacement. Because of the apparent antiquity of the Anderson Creek fault (see below), the Cool Gulch fault may also be an old (Mesoproterozoic) structure.

ANDERSON CREEK FAULT

The Anderson Creek fault is mapped across the southeast corner of the map south into the Gibbonsville quadrangle (Stewart and others, 2014) and the North Fork quadrangle (Lonn and others, 2013). The northern extent of the fault is uncertain. We show it being truncated by the Pierce Creek fault, but it may instead be intruded out by the *Tmbg* unit. The mafic intrusion that appears to have intruded along the fault has been provisionally dated at ~1,260-1,270 Ma (see *Ymi* description above). If the date is correct, this structure had a long history. Both dextral and down-on-the-west normal slip was proposed by Stewart and others (2014) based on stratigraphic arguments and 11 km (7 mi) offset between the Lick Creek fault contact of *Ys* with *Yqcs* in the Gibbonsville quadrangle and the Cool Gulch fault contact of *Yg* with *Yqcs* near the south edge of this map. The dissimilarity of those contacts makes them a poor piercing point, however. Stewart and others (2014) also cited Bacorn (1905) and Mayerle and Close (1993) for evidence from underground mines in the Gibbonsville area that indicated right-lateral strike-slip motion. Post-Eocene dip-slip motion is supported by the presence of Challis Volcanic Group strata west of the fault in the Gibbonsville and North Fork quadrangles (Stewart and others, 2014; Lonn and others, 2013). Net slip depends on the stratigraphic position of *Yqcs* versus *Yg*.

PIERCE CREEK FAULT

The Pierce Creek fault is mapped as a northeast-striking structure in the southern part of the quadrangle. Its northeastern extension is uncertain but we have tentatively shown it to be the northern terminus of the Anderson Creek fault. Its northeastern trace is based on field relations east of the map.

CAMP CREEK FAULT

The Camp Creek normal fault strikes southwest and dips northwest across the northwest part of the quadrangle. Along part of its trace, it is the northwest contact of the quartz syenite unit (*Tqs*). Northwest of it the Eocene dike swarm is dominated by rhyolite (*Tdsr*), as opposed to the dacite-dominated dike swarm to the southeast (*Tds*). It appears to mark a transition from more north-trending faults north of this quadrangle to a northeast structural grain crossing the central part of the Lost Trail Pass quadrangle.

MINERALIZATION

Several prospects are present in the quadrangle, but no significant amount of mining has taken place. Unpublished maps and documents for mining properties are available by examining "Property Details" through the interactive map ("Mines" web app) on the Idaho Geological Survey website (https://www.idahogeology.org/webmap). Property code (e.g., DI0001) is given below to assist with website searches.

KOPER KYUTE PROSPECT (DI0001)

The Koper Kyute prospect in the south-central part of the quadrangle is developed by an upper trench and a lower pit that exposes a northwest-southeast zone of probable calc-silicate rock with local copper stain. Exposures in the lower pit were initially thought to be dike, but thin section examination indicates that hornblende, quartz, and epidote are the primary minerals and titanite, plagioclase, pyroxene, and calcite are minor constituents. Rock has varied and high magnetite content. Median magnetic susceptibility from 15 measurements (Yqcs-KK, Table 1) is 16.19×10^{-3} SI; the highest reading of $1{,}732 \times 10^{-3}$ SI shows that about half of that rock measured is magnetite (reference data from Hunt and others, 1995). Possibly a magnetite skarn zone. One of two samples from the lower pit has an anomalous Cu concentration (1,716 ppm; 23RL028a, Table 2). Although no intrusive rocks are present at the lower pit, minor felsic intrusive float was found in the upper trench and there could be additional intrusions at depth related to the nearby *Td* and *Tr* dikes and the dike swarm (*Tds*) to the northwest.

REFERENCES

Bacorn, H.C., 1905, A complicated fault-system: The Engineering and Mining Journal, v. 79, p. 324.

Burmester, R.F., Lewis, R.S., Othberg, K.L., Stanford, L.R., Lonn, J.D., and McFaddan, M.D., 2016a, Geologic map of the western part of the Salmon 30 x 60-minute quadrangle, Idaho and Montana: Idaho Geological Survey Geologic Map 52, scale 1:75,000.

Burmester, R.F., Lonn, J.D., Lewis, R.S., and McFaddan, M.D., 2016b, Stratigraphy of the Lemhi subbasin of the Belt Supergroup, *in* MacLean, J.S., and Sears, J.W., eds., Belt Basin: Window to Mesoproterozoic Earth: Geological Society of America Special Paper 522, p. 121-137.

Burmester, R.F., Lewis, R.S., Lonn, J.D., and McFaddan, M.D., 2023, Lemhi subbasin stratigraphy and structure: an update: Northwest Geology, v. 52, p. 11-28.

Desmarais, N.R., 1983, Geology and geochronology of the Chief Joseph plutonic-metamorphic complex, Idaho-Montana: University of Washington Ph.D. dissertation, 19 p., scale 1:100,000.

Ekren, E.B., 1988, Stratigraphic and structural relations of the Hoodoo Quartzite and Yellowjacket Formation of Middle Proterozoic age from Hoodoo Creek eastward to Mount Taylor, central Idaho: U.S. Geological Survey Bulletin 1570, 17 p.

Elliott, C.G., Lonn, J.D., and Salazar, R., in prep., Geologic Map of the West Half of the Wisdom 30' x 60' Quadrangle: MBMG Open-File Report, one plate.

Evans, K.V., and Green, G.N., 2003, Geologic map of the Salmon National Forest and vicinity, east-central Idaho: U.S. Geological Survey Geologic Investigations Series Map I-2765, 19 p., scale 1:100,000.

Fisher, F.S., McIntyre, D.H., and Johnson, K.M., 1992, Geologic map of the Challis quadrangle, Idaho: U.S. Geological Survey Miscellaneous Investigations Series Map I-1819, scale 1:250,000.

Hobbs, S.W., 1980, The Lawson Creek Formation of Middle Proterozoic age in east-central Idaho: U.S. Geological Survey Bulletin 1482-E, 12 p.

Hunt, C.P., Moskowitz, B.M, and Banerjee, S.K., 1995, Magnetic properties of rocks and minerals, *in* Ahrens, T.J., ed., Rock Physics & Phase Relations: A Handbook of Physical Constants, Volume 3. https://doi.org/10.1029/RF003p0189.

Lane, E.W., 1947, Report of the subcommittee on sediment terminology: Transactions of the American Geophysical Union, v. 28, no. 6, p. 936-938.

Le Bas, M.J., and Streckeisen, A.L., 1991, The IUGS systematics of igneous rocks: Journal of the Geological Society of London, v. 148, p. 825-833.

Lonn, J.D., Othberg, K.L., Lewis, R.S., Burmester, R.F., Stanford, L.R., and Stewart, D.E., 2013, Geologic map of the North Fork quadrangle, Lemhi County, Idaho and Beaverhead County, Montana: Idaho Geological Survey Digital Web Map 160, scale 1:24,000.

Lonn, J.D., Elliott, C.G., Lewis, R.S., Burmester, R.F., McFaddan, M.D., Stanford, L.R., and Jänecke, S.U., 2019, Geologic map of the Montana part of the Salmon 30' x 60' quadrangle, southwestern Montana: Montana Bureau of Mines and Geology Geologic Map 75, 28 p., 1 sheet, scale 1:100,000.

Lonn, J.D, and Scarberry, K.C., 2022, Geologic Map of the Odell Lake 7.5' Quadrangle, southwestern Montana: Montana Bureau of Mines and Geology Geologic Map 86, scale 1:24,000, 1 sheet.

Lorain, S.H., and Metzger, O.H., 1939, Reconnaissance of placer-mining districts in Lemhi County, Idaho: U.S. Bureau of Mines Information Circular 7082, 81 p.

Ludwig, K.R., 2003, User's Manual for Isoplot 3.0: Berkeley Geochronology Center, Berkeley, California, 70 p.

Mayerle, R.T., and Close, T.J., 1993, Mineral investigation of the Anderson Mountain study area, Lemhi County Idaho: U. S. Bureau of Mines, Mineral Land Assessment Open File Report 25-93, 36 p.

McKee, E.D., and Weir, G.W., 1953, Terminology for stratification and cross-stratification in sedimentary rocks: Geological Society of America Bulletin, v. 64, p. 381-390.

Mosolf, J.G., Hanson, A., McDonald, K., Parker, S., and Scarberry, K., 2023, Major oxide and trace element analyses of rock samples collected in the Dillon and Wisdom 30' x 60' quadrangles, southwest Montana: Montana Bureau of Mines and Geology Analytical Dataset 1.

Mosolf, J.G., and Kylander-Clark, A., 2023a, U-Pb geochronology data from rock samples collected in the Dillon, Hamilton, Philipsburg, Townsend, and Wisdom 30' x 60' quadrangles, western Montana, 2020-2021: Montana Bureau of Mines and Geology Analytical Dataset 3.

Mosolf, J.G., and Kylander-Clark, A., 2023b, U-Pb geochronology data from rock samples collected in the Dillon and Wisdom 30' x 60' quadrangles, western Montana, 2021-2022: Montana Bureau of Mines and Geology Analytical Dataset 4.

Spitzer, M., Wildenhain, J., Rappsilber, J., and Tyers, M., 2014, BoxPlotR: a web tool for generation of box plots: Nature Methods volume 11, pages 121–122.

Stewart, E.D., Steel T.D., Stewart D.E., and Link, P.K., 2014, Geologic map of Gibbonsville, Shewag Lake, and Allan Mountain quadrangles, and parts of the Lost Trail Pass and Big Hole Pass quadrangles, Lemhi County, Idaho, and Ravalli and Beaverhead counties, Montana: Idaho Geological Survey Technical Report 14-2, scale 1:40,000.

Stewart, D.E., Lewis, R.S., Burmester, R.F., and Lonn, J.D., in prep, Geologic map of the Gibbonsville quadrangle, Lemhi County, Idaho, and Beaverhead County, Montana: Idaho Geological Survey Digital Web Map DWM-000, scale 1:24,000.

Walker, J.D., and Geissman, J.W., compilers, 2022, Geologic Time Scale v. 6.0: Geological Society of America. doi: 10.1130/2022.CTS006C.

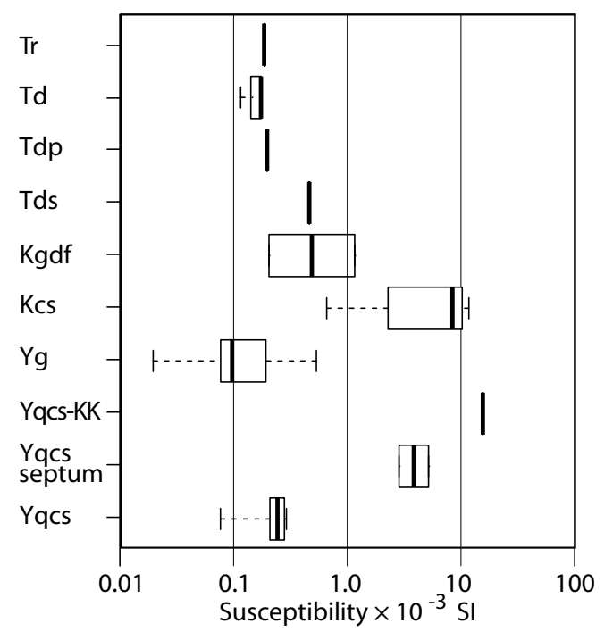

Figure 2. Box plot (Spitzer and others, 2014) of magnetic susceptibilities for map units measured. Yqcs-KK is for Koper Kyute prospect. Susceptibility (x) axis is logarithmic. Bold black lines show the medians; box limits are the 25th and 75th percentiles; whiskers extend to minimum and maximum values. See Table 1 for data for each unit. Base plot generated using http://shiny.chemgrid.org/boxplotr/.

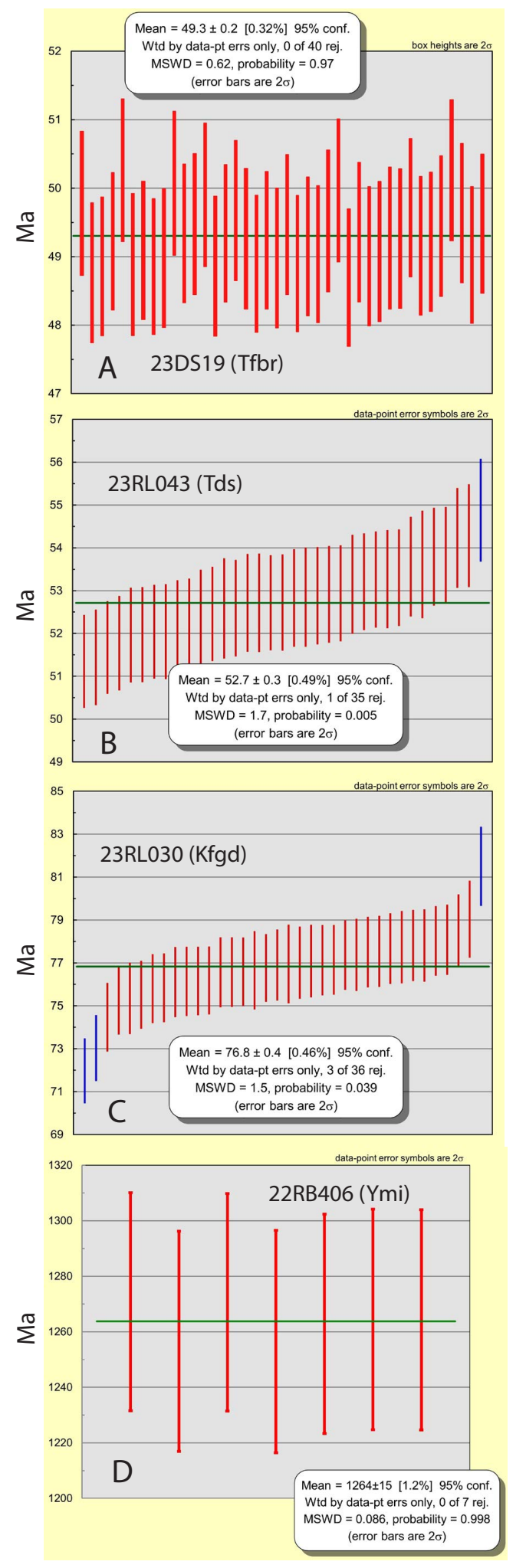

Figure 3. Weighted mean plots of LA-ICPMS U-Pb ages from igneous zircons. Analytical work by Stuart Parker and Dan Brennan of the Montana Bureau of Mines and Geology using facilities at University of California, Santa Barbara. Plotted using Ludwig (2003). Sample locations (NAD27): 23DS19 = 45.7188, -113.9910; 23RL043 = 45.6788, -113.9637; 23RL030 = 45.6723, -113.9532; 22RB406 = 45.6203, -113.8921.

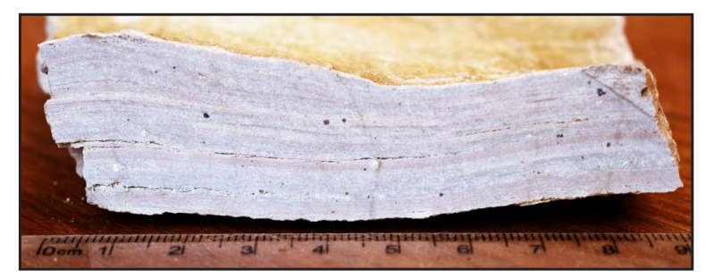

Figure 4. Flow-banded rhyolite (*Tfbr*) collected from west of Saddle Mountain in the northwest part of the quadrangle (sample 23DS19). Sample dated by U-Pb zircon methods (Figure 3A).

Figure 5. Biotite dacite tuff (*Tbdt*) from south-southwest of Saddle Mountain.

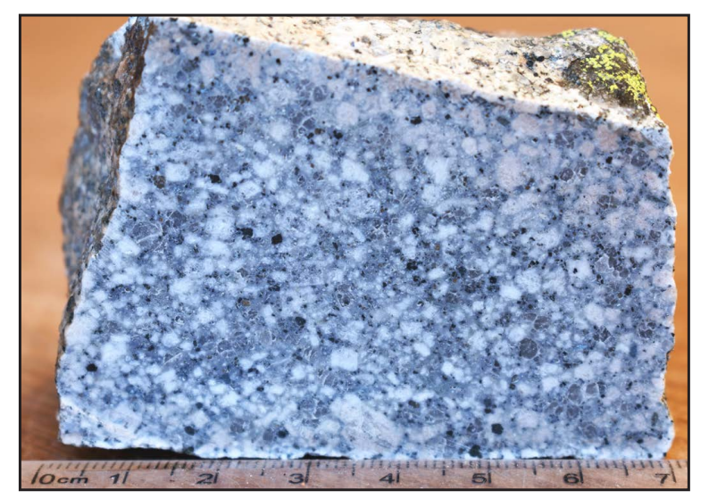

Figure 6. Porphyritic dacite dike (*Tds*) or stock collected from about 2.2 km (1.4 mi) southwest of Lost Trail Pass (sample 23RL043) and dated by U-Pb methods (Figure 3B).

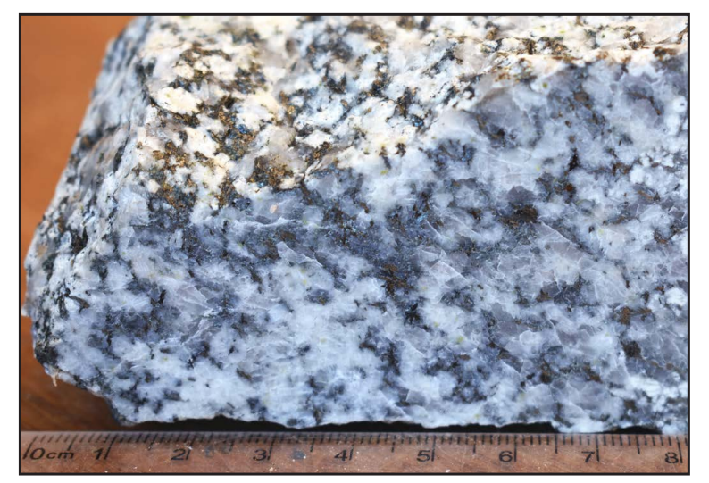

Figure 7. Foliated biotite granodiorite (*Kgdf*) collected from roadcut along U.S. Highway 93 about 2.4 km (1.5 mi) south-southwest of Lost Trail Pass and dated by U-Pb methods (sample 23RL030, Figure 3C).

Figure 8. Calc-silicate vein or dike (*Kcs*) northwest of Pierce Creek about 0.9 km (0.5 mi) from the southern map boundary.

Figure 9. Calc-silicate rocks of the *Yqcs* unit north of the Cool Gulch fault.

Figure 10. Folds in a loose block from the hanging wall of the Cool Gulch fault west of U.S. Highway 93. Nearby outcrop shows that small folds in fine schist and thin quartzite plunge south-southwest.

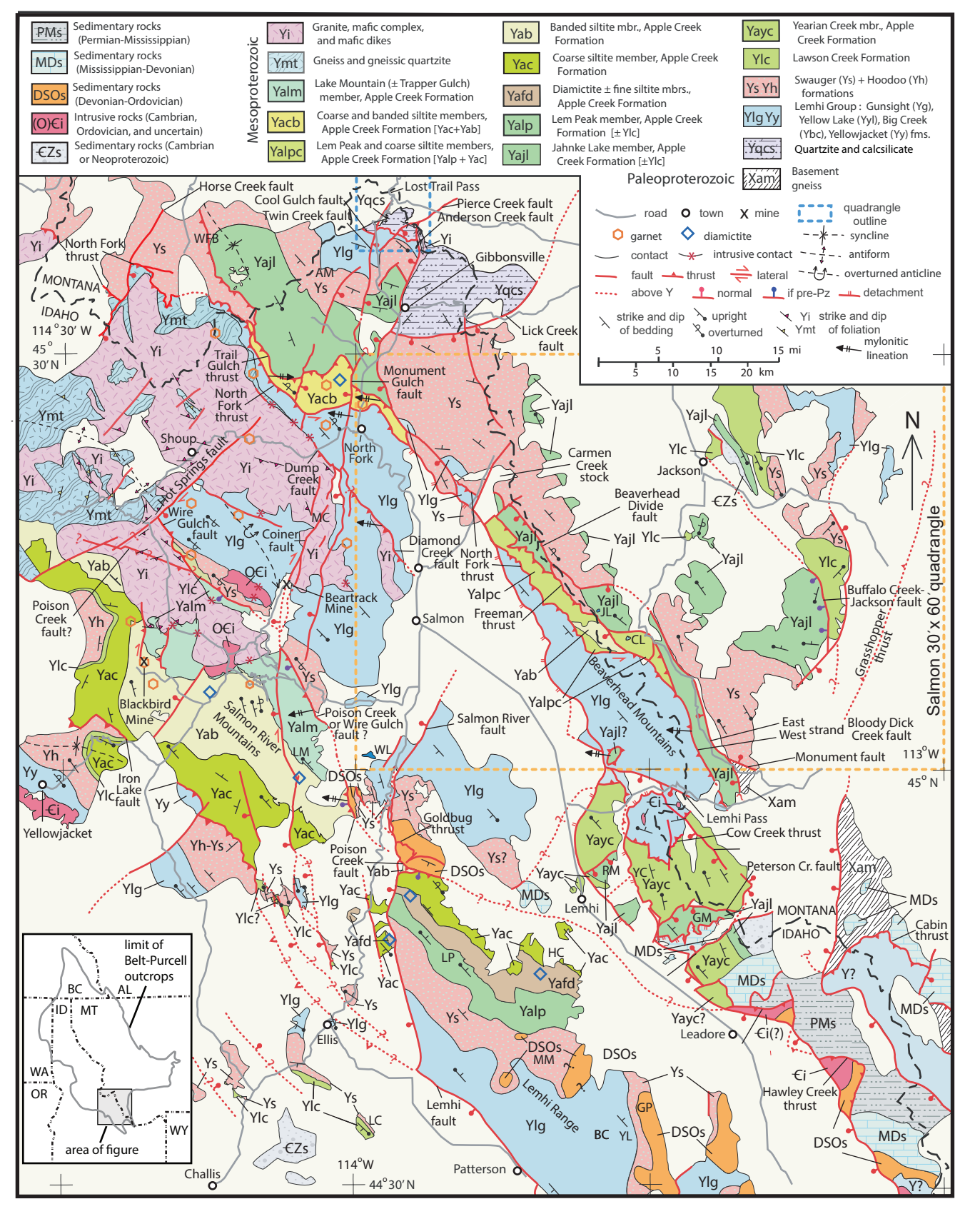

Figure 1. Pre-Mesozoic bedrock geology around Salmon, Idaho. The coarsest clastic unit (Ys = Yh) separates lower formations of the Lemhi Group (in blue) from higher Lawson Creek and Apple Creek formations (greens and yellows). Units are combined where scale or previous mapping makes separating them impractical. Geographic locations are in italics: AM—Allan Mountain; BC—Big Creek; CL—Cowbone Lake; GM—Goat Mountain; GP—Gunsight Peak; HC—Hayden Creek, JL—Jahnke Lake; LC—Lawson Creek; LM—Lake Mountain; LP—Lem Peak; MC—Moose Creek; MM—Mogg Mountain; RM—Ramsey Mountain; WFB—West Fork Bitterroot River; YC—Yearian Creek; YL—Yellow Lake. Dashed rectangles outline the Salmon 1° x 2° (orange) and Lost Trail Pass (blue) maps. Modified after Burmester and others (2023) to include insights from field work in 2023.

Table 1. Magnetic susceptibility measurements of rocks in the Lost Trail Pass quadrangle. Values determined from hand specimens or rock faces as measured with KT-9 and KT-10 Kappameters from Exploranium G.S. Ltd. and Terraplus Inc., typically on 10 measurements per exposure and averaged and reported in SI units (x 10^{-3}).

Measurement ID	Map unit	Latitude	Longitude	Median	Average	Std_Dev	N
23RBms0448	Tr	45.6672	-113.9374	0.193	0.190	0.029	1
23RBms0462	Td	45.6729	-113.9518	0.181	0.185	0.045	7
23RBms0450	Td	45.6668	-113.9364	0.183	0.182	0.011	5
23RBms0554	Tdp	45.6359	-113.9822	0.222	0.238	0.030	5
22RBms002	Kgdf	45.6723	-113.9531	0.213	0.275	0.207	8
22RBms001	Tds	45.6714	-113.9508	0.482	0.734	0.692	6
23RBms0461	Kgdf	45.6722	-113.9532	1.208	1.455	1.097	17
23RBms0553cs	Kcs	45.6386	-113.9830	0.685	1.277	1.438	8
23RBms0514	Kcs	45.6309	-113.9923	8.228	10.457	8.538	12
23RBms0516	Kcs	45.6321	-113.9934	9.303	13.140	11.029	15
12DS68	Kcs	45.6329	-113.9574	12.200	14.897	15.828	3
07RL591	Yg	45.6439	-113.9707	0.020	0.020		1
12DS70	Yg	45.6479	-113.9522	0.060	0.060		1
12MDM068	Yg	45.6471	-113.9568	0.060	0.060		1
12MDM070	Yg	45.6463	-113.9588	0.070	0.070		1
12DS74	Yg	45.6436	-113.9558	0.080	0.080		1
23RBms0535	Yg	45.6269	-113.9819	0.096	0.105	0.068	11
12DS69	Yg	45.6476	-113.9522	0.100	0.100		1
12RL238	Yg	45.6410	-113.9701	0.100	0.100		1
23RBms0513	Yg	45.6290	-113.9895	0.101	0.105	0.048	15
12DS73	Yg	45.6497	-113.9511	0.110	0.110		1
23RBms0518	Yg	45.6325	-113.9953	0.113	0.114	0.029	10
23RBms0551	Yg	45.6459	-113.9834	0.136	0.134	0.074	10
12MDM066	Yg	45.6493	-113.9602	0.200	0.200		1
23RBms0553q	Yg	45.6386	-113.9830	0.225	1.135	3.275	15
23RBms0549	Yg	45.6479	-113.9847	0.361	0.376	0.200	7
12RL239	Yg	45.6389	-113.9693	0.390	0.390		1
23RBms0517	Yg	45.6326	-113.9931	0.556	1.233	1.637	15
23RBms0454	Yqcs-KK	45.6635	-113.9374	16.187	171.544	448.124	15
23RBms0459	Yqcs septum	45.6828	-113.9433	2.966	6.535	8.504	20
22RBms003	Yqcs septum	45.6630	-113.9616	5.389	5.635	4.151	13
23RBms0457	Yqcs	45.6609	-113.9427	0.080	0.079	0.012	10
12DS72	Td	45.6511	-113.9503	0.120	0.120		1
22RBms004b	Yqcs	45.6555	-113.9714	0.201	0.197	0.070	11
23RBms0451	Yqcs	45.6648	-113.9383	0.217	0.237	0.094	15
12DS71	Yqcs	45.6520	-113.9509	0.250	0.250		1
23RBms0548	Yqcs	45.6479	-113.9846	0.253	0.252	0.069	12
22RBms006	Yqcs	45.6448	-113.9706	0.253	0.259	0.074	10
23RBms0455	Yqcs	45.6632	-113.9373	0.291	0.259	0.095	15
23RBms0449	Yqcs	45.6669	-113.9365	0.300	0.307	0.037	9
22RBms005	Yqcs	45.6485	-113.9704	0.303	0.340	0.131	15

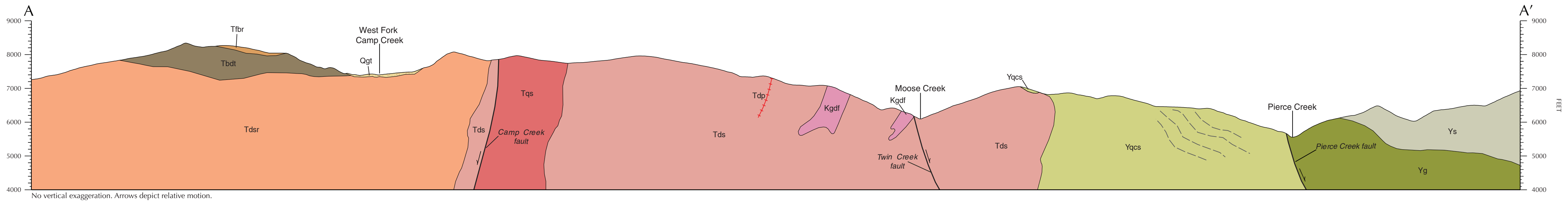

No vertical exaggeration. Arrows depict relative motion.

Table 2. Major-oxide and trace-element analyses of samples collected in the Lost Trail Pass quadrangle and nearby areas. Analyses performed by X-ray fluorescence methods at Washington State University. Coordinate datum NAD27.

Sample	Latitude	Longitude	Unit name	Map unit	Quadrangle	SiO2	TiO2	Al2O3	FeO*	MnO	MgO	CaO	Na2O	K2O	P2O5	Sum	LOI %	Ni	Cr	Sc	V	Ba	Rb	Sr	Zr	Y	Nb	Ga	Cu	Zn	Pb	La	Ce	Th	Nd	U
23RL028a	45.6635	-113.9375	Quartzite and calc-silicate rocks	Yqcs	Lost Trail Pass	69.59	0.111	2.17	15.09	0.197	3.53	4.54	0.22	0.16	0.008	95.62	4.03	12	17	6	62	859	1	37	47	82	0.7	3	1716	56	3	78	164	5	76	0
23RL028b	45.6635	-113.9375	Quartzite and calc-silicate rocks	Yqcs	Lost Trail Pass	50.68	0.337	7.78	13.52	0.499	9.96	12.53	0.91	0.80	0.048	97.07	2.60	35	40	13	77	98	16	67	106	14	3.4	[illegible]	[illegible]	[illegible]	[illegible]	[illegible]	[illegible]	[illegible]	[illegible]	[illegible]
23RL030	45.6723	-113.9532	Foliated granodiorite	Kgdf	Lost Trail Pass	69.70	0.359	15.35	2.70	0.060	0.99	3.34	3.89	2.29	0.109	98.79	1.08	6	13	4	38	1043	69	512	169	12	10.8	[illegible]	[illegible]	[illegible]	[illegible]	[illegible]	[illegible]	[illegible]	[illegible]	[illegible]
22RB402	45.6106	-113.7933	Muscovite-biotite granite	Tmbg	Big Hole Pass	71.58	0.242	14.87	1.98	0.084	0.59	2.10	3.86	3.27	0.094	98.67	0.88	5	7	4	26	763	107	271	102	22	15.7	[illegible]	[illegible]	[illegible]	[illegible]	[illegible]	[illegible]	[illegible]	[illegible]	[illegible]
22LK008	45.5365	-113.8280	Mafic intrusive rocks?	Ymi?	Big Hole Pass	50.77	1.039	12.77	10.07	0.171	10.05	9.98	1.44	1.05	0.088	97.44	2.15	218	671	33	274	246	42	126	88	21	4.2	[illegible]	[illegible]	[illegible]	[illegible]	[illegible]	[illegible]	[illegible]	[illegible]	[illegible]
22RB406	45.6203	-113.8921	Mafic intrusive rocks	Ymi	Gibbonsville	52.67	1.474	12.75	10.42	0.149	8.45	9.38	2.20	1.21	0.152	98.85	1.05	170	436	28	285	214	46	256	120	20	7.6	[illegible]	[illegible]	[illegible]	[illegible]	[illegible]	[illegible]	[illegible]	[illegible]	[illegible]

Published and sold by the Idaho Geological Survey
University of Idaho, Moscow, Idaho 83844-3014